

## Microscopic picture of Co clustering in ZnO

Diana Iușan,<sup>1</sup> Mukul Kabir,<sup>2</sup> Oscar Grånäs,<sup>1</sup> Olle Eriksson,<sup>1</sup> and Biplab Sanyal<sup>1,\*</sup>

<sup>1</sup>*Department of Physics and Materials Science, Uppsala University, P.O. Box 530, SE-75121 Uppsala, Sweden*

<sup>2</sup>*Department of Materials Science and Engineering, Massachusetts Institute of Technology, Cambridge, Massachusetts 02139, USA*

(Received 5 November 2008; revised manuscript received 30 January 2009; published 16 March 2009)

Density functional theory was applied to study the chemical and magnetic interactions between Co atoms doped in ZnO. It was found that the Co impurities tend to form nanoclusters and the interactions between these atoms are antiferromagnetic within the local spin-density approximation (LSDA)+Hubbard  $U$  approach. The extracted interatomic exchange parameters agree reasonably well with recent experimental results. We have analyzed and compared the electronic structure obtained using the LSDA and LSDA+ $U$  approaches and found that the LSDA+ $U$  gives the most reasonable result, highlighting the importance of short-ranged antiferromagnetic interactions due to superexchange.

DOI: 10.1103/PhysRevB.79.125202

PACS number(s): 75.50.Pp, 75.70.-i, 71.70.Gm

### I. INTRODUCTION

A tremendous research effort in the past years has been dedicated to the study of diluted magnetic semiconductors (DMSs) due to their potential applications in semiconductor spintronics. A major obstacle to obtain an undisputed diluted ferromagnetic (FM) semiconductor at room temperature from the pool of widely varied experimental results has been identified as the inhomogeneous distribution of magnetic dopants.<sup>1,2</sup> Among the magnetically doped wide band-gap oxides, Co:ZnO is still intriguing regarding the coupling of magnetism with the structural and electrical properties. Ferromagnetism has been observed in Co:ZnO films in the superconducting quantum interference device (SQUID) measurements, although x-ray magnetic circular dichroism (XMCD) revealed a paramagnetic Co sublattice.<sup>3,4</sup> Iușan *et al.*<sup>4</sup> showed that the observed paramagnetism in 5% Co in ZnO is due to the presence of Co nanoclusters. Also, by successive annealings in O<sub>2</sub> atmosphere, the ferromagnetism of Co:ZnO nanoparticles could be correlated with the presence of defects.<sup>5</sup> Before any claims of intrinsic ferromagnetism can be made, an extremely careful structural analysis must be done to exclude the presence of secondary phases<sup>6</sup> or nanocrystals<sup>7</sup> that can account for the observed ferromagnetism. This issue becomes even more acute in DMSs with low concentrations of magnetic transition metals (typically ~5%). Recently, Dietl *et al.*<sup>8</sup> explained ferromagnetism as arising from uncompensated spins at the surface of Co-rich antiferromagnetic (AFM) nanoclusters embedded in a Co-poor ZnO host. Prior to Ref. 8, it was argued that inhomogeneities of the lattice in the form of magnetic clusters lead to superparamagnetism or weak ferromagnetism due to uncompensated spins at the surfaces of the clusters within which the interactions among the atoms are antiferromagnetic.<sup>9,10</sup>

In this study we address a key problem of diluted magnetic semiconductors: namely, how does the spatial arrangement of the magnetic dopants within the semiconducting matrix affect the exchange interactions among them. We show from first-principles calculations that the Co nanoclusters in ZnO show interatomic antiferromagnetic exchange interactions which produce a net magnetic moment which is either zero or a small number.

### II. COMPUTATIONAL DETAILS

We have performed calculations using the density-functional theory (DFT), within the projector augmented-wave method<sup>11</sup> and Perdew-Burke-Ernzerhof exchange-correlation functional,<sup>12</sup> as implemented in the VASP package.<sup>13</sup> The effects of strong electron-electron interactions have been taken into account using the approach of Dudarev *et al.*<sup>14</sup> to local spin-density approximation (LSDA)+ $U$ . A value of  $U=5$  eV was used for the Coulomb interaction parameter, while the exchange parameter  $J$  was set to 1 eV. This choice for  $U$  and  $J$  provides a good agreement between the experimental and theoretical spectra, as we have shown in a previous study.<sup>15</sup> Similar values have been used in other theoretical calculations on these compounds following the LSDA+ $U$  approach.<sup>16</sup> The wave functions were expanded in a plane-wave basis set with the kinetic-energy cutoff of 500 eV. The wurtzite lattice constants were set to  $a=3.25$  Å and  $c=5.21$  Å. In order to test the structural stability of the clusters, supercells of different sizes have been used: 32 atoms ( $2a \times 2a \times 2c$ ), 72 atoms ( $3a \times 3a \times 2c$ ), 108 atoms ( $3a \times 3a \times 3c$ ), and 144 atoms ( $3a \times 3a \times 4c$ ). The geometry of the system was optimized until the forces were less than 0.01 eV/Å. All our calculations refer to collinear spin structures. According to the general consensus, we have considered that Co substitutes the cation (Zn) site. The size of the clusters ranges from 1 to 4. For each of the supercells studied, different structural and magnetic configurations are schematically shown in Fig. 1.

The orbital moment was calculated using the full potential augmented plane-wave package EXCITING.<sup>17</sup> The orbital moment was converged for basis set cutoffs corresponding to  $R_{\text{MT}}G_{\text{max}}=8.0$ , with muffin-tin radius  $R_{\text{MT}}=1.919$  Å, and a Brillouin-zone sampling of 175 points for 16 atoms. The electronic correlation was treated within the most general version of LDA+ $U$ ,<sup>18</sup> as implemented in Ref. 19, with the fully localized limit as double counting.<sup>20</sup> The  $U$  and  $J$  parameters were chosen to be 5 and 1 eV, respectively.

### III. RESULTS

#### A. Structural and magnetic properties

In order to discuss the chemical and magnetic stability of different Co geometries, we introduce a vector with six ele-

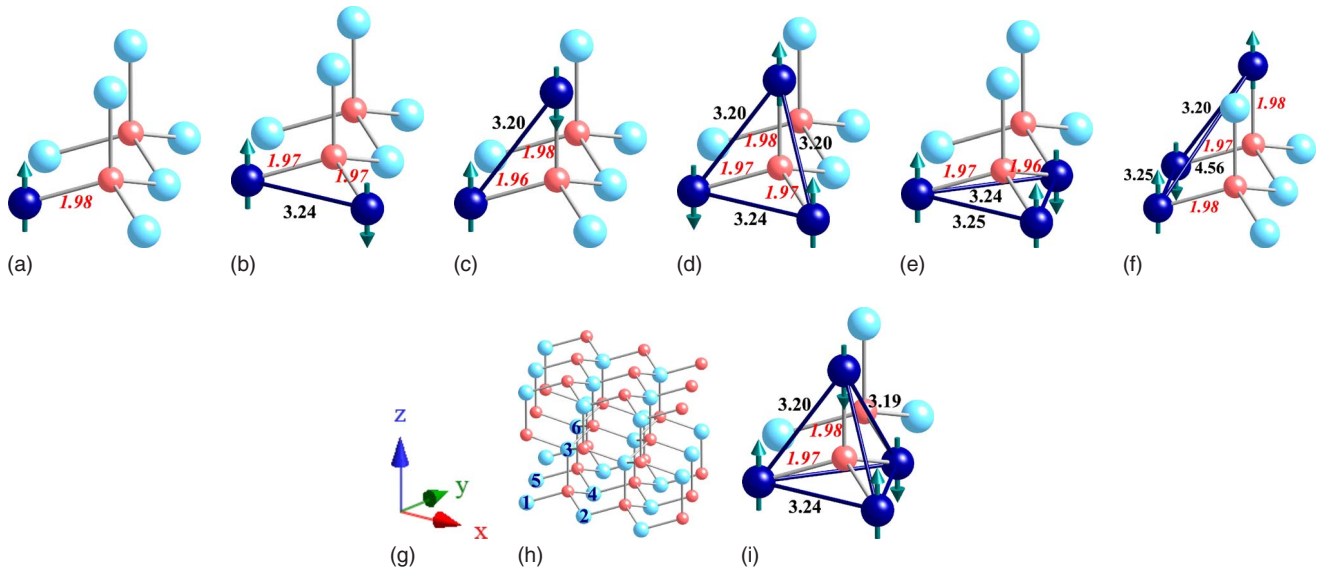


FIG. 1. (Color online) Schematic illustrations of the Co clusters in the ZnO matrix for various cluster sizes and configurations. Co, Zn, and O atoms are shown as blue (dark), turquoise light), and red (small gray) colored balls, respectively. The bond lengths calculated by LSDA+ $U$  method are shown. Magnetic configurations are evident from the arrows connected with the Co atoms.

ments. The components of this vector correspond to the chemical occupancies at different sites in the ZnO matrix, as denoted in Fig. 1(g). Additional arrows are introduced to illustrate the corresponding magnetic coupling between the Co atoms when relevant for the discussion. For example, two Co atoms substituting for Zn in the  $(xy)$  plane of the lattice, the sites numbered with 1 and 4 in Fig. 1(g), would have the characterizing vector (Co,Zn,Zn,Co,Zn,Zn). If we further assumed an antiferromagnetic coupling between the magnetic atoms, we would describe the situation by the vector  $(\uparrow, \cdot, \cdot, \downarrow, \cdot, \cdot)$ .

First, let us analyze the case of a single Co atom substitutional at a cation site. Its structure is shown in Fig. 1(a), and it can be represented by the vector (Co,Zn,Zn,Zn,Zn,Zn). The Co atom has an approximately tetrahedral coordination with the O atoms and acquires a high magnetic moment of  $3.0\mu_B$ /atom. The Co impurity induces a positive spin polarization on the neighboring O atoms, which is halved within the LSDA+ $U$  ( $0.04\mu_B$ ) compared to LSDA ( $0.08\mu_B$ ). This can be attributed to the increased Co-O bond length in the LSDA+ $U$  case ( $1.98 \text{ \AA}$  vs  $1.96 \text{ \AA}$ ) as well as the modified electronic structure caused by the Hubbard  $U$ .

The addition of a second Co atom allows us to study the interactions among these atoms. For this purpose, we have increased the size of our supercell to involve 72 atoms, and we studied the stability of different structural and magnetic arrangements of the Co atoms. The most stable structure corresponds to the case where the Co atoms are nearest neighbors in the  $(xy)$  plane of the wurtzite lattice, the configuration which we shall refer to as *in plane* and which is represented in Fig. 1(b), characterized by the vector (Co,Co,Zn,Zn,Zn,Zn). For this structure the AFM state is the ground state  $(\uparrow, \downarrow, \cdot, \cdot, \cdot, \cdot)$ , with the FM state 11 (LSDA+ $U$ )/17 (LSDA) meV/Co atom higher in energy. The next most stable configuration is just 2 (LSDA+ $U$ )/2 (LSDA) meV/Co atom higher in energy, and again it corresponds to

nearest-neighboring Co atoms, this time oriented out of the  $(xy)$  plane, the configuration which we shall refer to as *out of plane* [see Fig. 1(c)] (Co,Zn,Co,Zn,Zn,Zn). For this structure the magnetic coupling is AFM within the LSDA+ $U$ , while a FM solution was found within the LSDA. The reason for this difference in exchange interaction from these two approximations becomes clear when we discuss the electronic structure of this system (below) and is caused by the fact that in the LSDA the (ferromagnetic) double exchange mechanism dominates whereas in LSDA+ $U$  the (antiferromagnetic) superexchange mechanism dominates.

The Co-Co distances corresponding to the out-of-plane and in-plane configurations are  $3.20$  and  $3.24 \text{ \AA}$ , respectively [see Figs. 1(b) and 1(c)]. The configuration with a larger Co-Co separation ( $4.57 \text{ \AA}$ ) lies higher in energy: 7 (LSDA+ $U$ )/34 (LSDA) meV/Co atom above the ground state, which indicates a tendency for clustering of the Co atoms in the ZnO host. The AFM and FM solutions are almost degenerate when the Co atoms are separated by this distance, indicating a very short-ranged character of the interatomic magnetic interactions. The tendency of clustering of the magnetic atoms is a general feature of transition-metal doped semiconductors,<sup>21</sup> and it motivates the study of trimers and tetramers, which we describe below.

In the case of the three Co atom clusters we have again examined different possible structures and spin arrangements of the Co atoms: FM, as well as all possible AFM configurations. Some of the analyzed geometries for the Co trimers and the corresponding magnetic ground-state configurations are represented in Figs. 1(d)–1(f). The structural ground state is a close triangular configuration, where the first two of the Co atoms are in the  $(xy)$  plane, while the third one is out of plane, as shown in Fig. 1(d). In accordance to the definition we gave above, we can describe this particular geometry with the help of the vector (Co,Co,Co,Zn,Zn,Zn); thus the Co atoms occupy the sites labeled 1–3 in Fig. 1(g).

The magnetic ground state corresponds to the case where the two in-plane atoms are coupled antiferromagnetically, while the out-of-plane atom couples antiferromagnetically with one of these in-plane atoms, i.e., the vector notation is  $(\uparrow, \downarrow, \uparrow, \cdot, \cdot, \cdot)$ . The FM state is 10 (LSDA+ $U$ )/16 (LSDA) meV/Co atom higher in energy. It is worth pointing out at this point that, within the LSDA+ $U$ , different geometrical distributions of the Co trimers, some shown in Figs. 1(d)–1(f), are separated by energies of just a few meV, making it hard to account for the true structure to be presented in experimental samples. Nevertheless, within the LSDA+ $U$ , the magnetic configuration of all considered structures corresponds to an antiferromagnetic one between the atoms in the ( $xy$ ) plane. Overall the results of the dimer and trimer suggest that (at least from LSDA+ $U$ ) antiferromagnetic interactions between the Co atoms dominate. The true magnetic ground state of the trimer is therefore expected to be a state close to a Néel state, with noncollinear spins which are aligned each with an angle close to  $120^\circ$  to the neighboring spins, as was, e.g., for instance analyzed in Ref. 22. A further analysis of this was, however, not pursued here.

For the Co tetramers we have considered the close pyramidal structure as the most probable structure. Different spin configurations have been taken into account: FM together with different AFM configurations. The magnetic ground state corresponds to the  $(\uparrow, \uparrow, \downarrow, \downarrow, \cdot, \cdot)$  and  $(\uparrow, \downarrow, \downarrow, \uparrow, \cdot, \cdot)$  spin arrangements (which are degenerate in energy), with a total magnetic moment equal to zero. The geometry and spin configuration of the tetramer are indicated in Fig. 1(h). The magnetic configurations  $(\uparrow, \uparrow, \uparrow, \downarrow, \cdot, \cdot)$  and  $(\uparrow, \uparrow, \downarrow, \uparrow, \cdot, \cdot)$  have a higher energy. The FM state, with a magnetic moment of  $3.0\mu_B$ /Co atom, is the least favored and it lies 16 (LSDA+ $U$ )/35 (LSDA) meV/Co atom higher in energy compared to the ground state. Again, the AFM interactions among the Co atoms are expected to result in a noncollinear structure. For supported magnetic clusters with pyramidal arrangement, several such configurations have been identified.<sup>23</sup>

In regards to the structural relaxation, the Co-Co and Co-O distances have in general larger values within the LSDA+ $U$  compared to LSDA. Also, a change from a FM to an AFM alignment of the Co spins leads to a decrease in the Co-Co distances for the in-plane atoms, while to an increase for the out-of-plane atoms. The Co-O-Co angles are smaller in value (with  $2^\circ$ ) for the out-of-plane arrangement of the Co atoms as compared to the in-plane one.

The choice of the exchange-correlation functional used was proven to be crucial for the determination of the intra-atomic magnetic interactions. In order to illustrate this effect we have plotted in Fig. 2 the energy difference between different antiferromagnetic solutions and the corresponding ferromagnetic solution for different geometrical arrangements of the Co atoms and cluster sizes. A positive (negative) value of  $E^{\text{AFM}} - E^{\text{FM}}$  means that the Co spins align ferromagnetically (antiferromagnetically). The first thing to be observed is that within the LSDA there is a competition between ferromagnetic and antiferromagnetic interactions, and the alignment of the spins is dependent on the arrangement of the Co atoms. Within the LSDA+ $U$  method, on the contrary, the preferred magnetic solution is always an antiferromagnetic

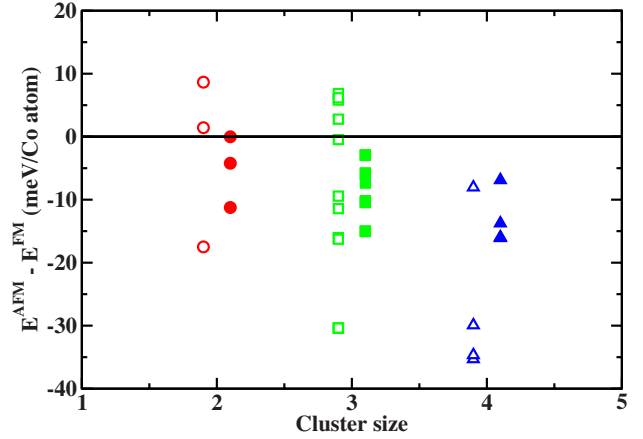


FIG. 2. (Color online) Dependence of the exchange interactions on the structure and cluster size. Filled symbols correspond to LSDA+ $U$  results and open symbols to LSDA results.

one. Second, the strength of the magnetic interactions is reduced within the LSDA+ $U$  calculations when compared to LSDA results. Our results are in good agreement with previous LSDA and LSDA+ $U$  studies of Co-doped ZnO.<sup>16</sup> The importance of a correct description of the electronic structure for the determination of the magnetic properties has been emphasized in other recent studies.<sup>24,25</sup> In addition, these studies suggest that the weak antiferromagnetic coupling observed in the undoped Co:ZnO could be turned to a ferromagnetic coupling by electron doping, the stabilization of the FM state being due to the partial occupation of the  $t_2$ -like minority bands. The connection between the electronic structure and the magnetic properties of transition-metal oxides has been discussed in more general terms by Solovyev.<sup>26</sup>

From the values of the total energies we can estimate the strength of the pair interactions,  $J_{ij}$ , between a Co atom on sites  $i$  and  $j$ , using an Ising-model Hamiltonian. The values are presented in Table I. Within LSDA, the in-plane interactions are antiferromagnetic and increase with increasing cluster size, while the out-of-plane interactions change from being FM for smaller cluster sizes to being AFM for larger sizes of the clusters. Within the LSDA+ $U$ , both the in-plane and out-of-plane magnetic interactions are antiferromagnetic and their strength is more or less independent of the Co cluster size. From magnetic measurements, exchange parameters  $J_{\text{in}} = -21$  K and  $J_{\text{out}} = -9$  K were reported,<sup>27</sup> which are in good agreement with our LSDA+ $U$  values, especially for the  $J_{\text{in}}/J_{\text{out}}$  ratio. A good consensus exists also with the the-

TABLE I. Exchange interaction parameters of an Ising Hamiltonian describing the magnetic interactions among the Co atoms within the cluster.

	$J$ (K)	Dimer	Trimer	Tetramer
LSDA	$J_{\text{in}}$	-45	-59	-74
	$J_{\text{out}}$	22	-1	-14
LSDA+ $U$	$J_{\text{in}}$	-29	-29	-30
	$J_{\text{out}}$	-11	-11	-12

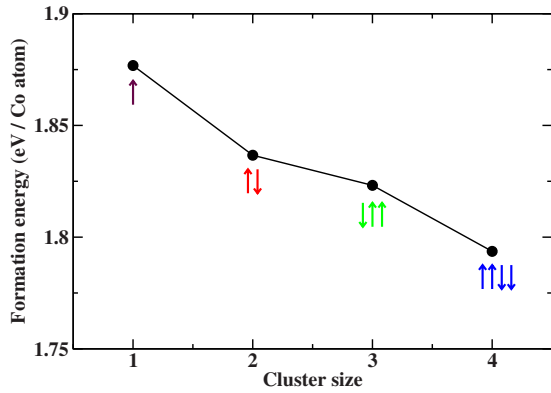


FIG. 3. (Color online) Formation energy as a function of the size of Co cluster for the corresponding ground-state magnetic configurations.

oretical calculations of Chanier *et al.*,<sup>28</sup> which reported the values of  $J_{\text{in}} = -23$  K and  $J_{\text{out}} = -8$  K for an isolated pair, with the LSDA+ $U$  approach.<sup>29</sup> In addition, very recent investigations of colloidal nanocrystals with a high Co content in a ZnO matrix indicate that the magnetic interactions among the Co atoms are antiferromagnetic.<sup>29</sup>

We have also calculated the formation energy of the cluster as

$$E^f = E[\text{Co}_m\text{Zn}_{N-m}\text{O}_N] - N * E[\text{ZnO}] - m * \{\mu[\text{Co}] - \mu[\text{Zn}]\},$$

where  $m$  and  $N$  are the number of Co and O atoms, respectively, and  $\mu$  is the chemical potential. A positive formation energy, according to this definition, means that it costs energy to incorporate Co in the ZnO matrix. The formation energy (within LSDA) of the Co clusters of different sizes is indicated in Fig. 3. As the cluster size increases, the formation energy decreases. Hence it costs less energy to substitute Co atoms for Zn if the Co atoms are close to each other. This shows that the Co atoms want to form clusters in the ZnO matrix. Similarly, a decrease in the formation energy with increasing cluster size has been observed for the Cr:GaN system.<sup>30</sup>

## B. Electronic structure

In Fig. 4, we show the density of states (DOS) for the monomer and the tetramer, within LSDA and LSDA+ $U$ . The addition of  $U$  on the Co 3d states pushes the majority bands into the valence band of the host. A pronounced effect on the Co minority states is observed where the sharp peak of  $e$  character at the Fermi level within LSDA is pushed close to the top of the valence band within LSDA+ $U$ . The splitting between the occupied and unoccupied minority Co states is  $\sim 4$  eV within the LSDA+ $U$ , an increase compared to the LSDA value. It is to be noticed that as the size of the cluster increases, the width of the Co bands increases. Also, a new peak appears below the Fermi level for the majority states (at  $\sim -0.5$  eV), and it is due to the hybridization of the Co atoms mediated by the O atom within the cluster. The electronic structure in Fig. 4 shows that the LSDA calculation results in a half-metallic state, which makes the ferromagnetic double exchange mechanism the dominant contribution to the interatomic exchange. The LSDA+ $U$  method results in a band gap at the Fermi level, and hence the antiferromagnetic superexchange mechanism dominates (a discussion of these mechanisms can be found, e.g., in Ref. 21). The electronic structure of oxide materials is often described better with the LSDA+ $U$  method, at least when compared to LSDA, and maybe the best example is the electronic structure of transition-metal oxides.<sup>31</sup> We believe that this is also the case here, but note that a careful comparison between calculated and measured valence-band spectra is the best way to decide which effective potential is the best for these systems. A recent experimental/theoretical study shone some light of this,<sup>4</sup> and it was concluded that the LSDA+ $U$  approach reproduced the measured valence-band spectrum with the best accuracy. This, together with our results here, suggests that Co-doped ZnO is dominated by short-ranged antiferromagnetic interactions for all Co cluster sizes.

For a visualization of the changes in the electronic structure due to clustering, we plot the magnetization density of a singly doped Co atom in Fig. 5 and that of a four-atom Co cluster in Fig. 6, both calculated within the LSDA+ $U$  method. The electron density was evaluated in energy intervals of 0.2 and 0.7 eV below the Fermi level, for the mono-

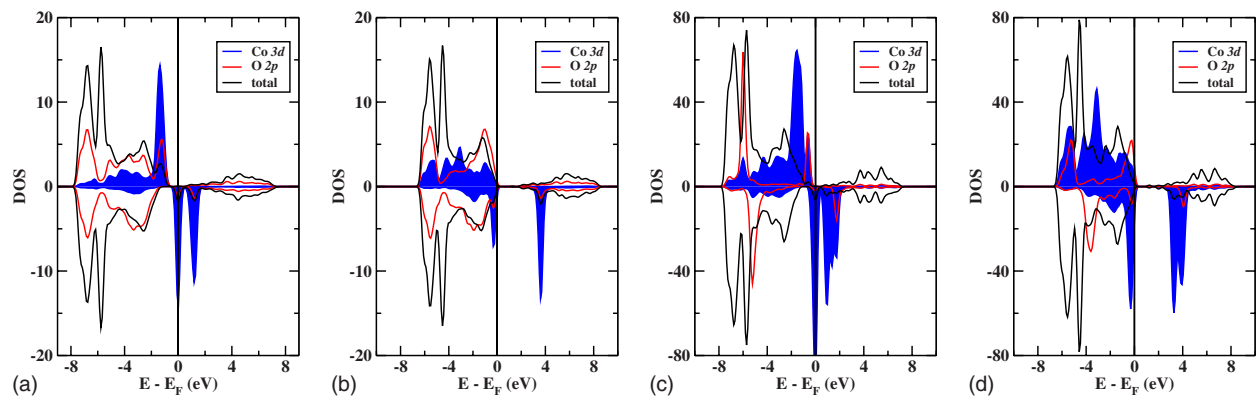


FIG. 4. (Color online) Calculated DOS for the Co monomer in the LSDA (a) and LSDA+ $U$  (b) and for the Co tetramer in the LSDA (c) and LSDA+ $U$  (d). The solid black (dark) line represents the total DOS, the blue shaded line stands for the Co 3d states, while the red (light) line is for the mediating O 2p states.



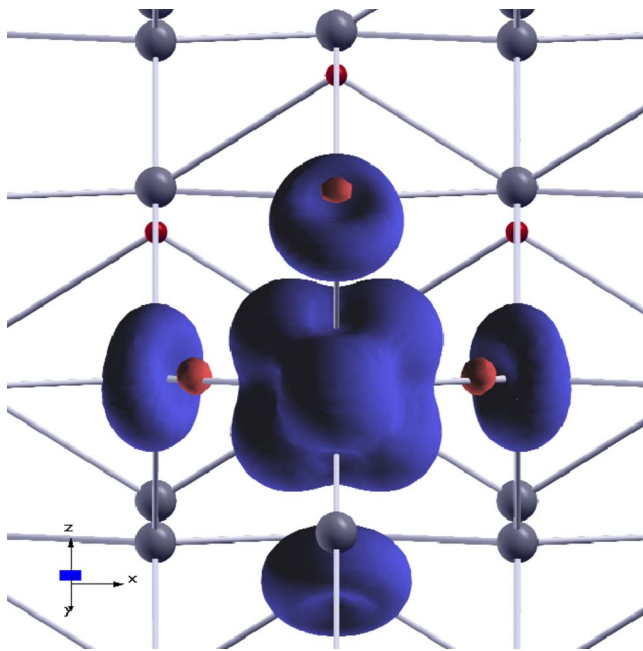


FIG. 5. (Color online) Magnetization density of a Co monomer in a ZnO matrix, evaluated within the LSDA+ $U$  for an energy interval of 0.2 eV below the Fermi level. Positive (negative) values of the magnetization density are represented in red (blue).

mer and the tetramer, respectively, to inspect the peak in the DOS due to clustering mentioned above. In accordance to the density-of-states plots (Fig. 4), it represents states in the energy interval where the occupied Co minority peak dominates, which is situated just below the Fermi level, and it is of approximately  $e$  character. This character is also reflected in the symmetry of the charge density in Figs. 5 and 6. It is, in this figure, also clear that some O  $p$  states are found in the energy intervals of 0.2/0.4 eV below  $E_F$  for the monomer and tetramer, respectively, which are consistent with Fig. 4. The character of the Co states is not changed by the clustering. We observe that the Co states induce a spin polarization on the neighboring O atoms. As a result of the clustering, the  $2p$  states of the mediating O atom are strongly perturbed, which changed the sign of the spin polarization of this atom (for this energy interval) as the number of surrounding Co atoms increases.

Since orbital magnetism can be quite important in Co based oxides, we have decided to also study this property. The orbital moment calculated for a Co monomer in a 16 atom cell (amounting to 12.5% Co on the Zn sublattice) is  $0.14\mu_B$ . This value is much smaller than the Co orbital moment in CoO in the NaCl structure, experimentally measured to be  $1.36\mu_B$ .<sup>32</sup>

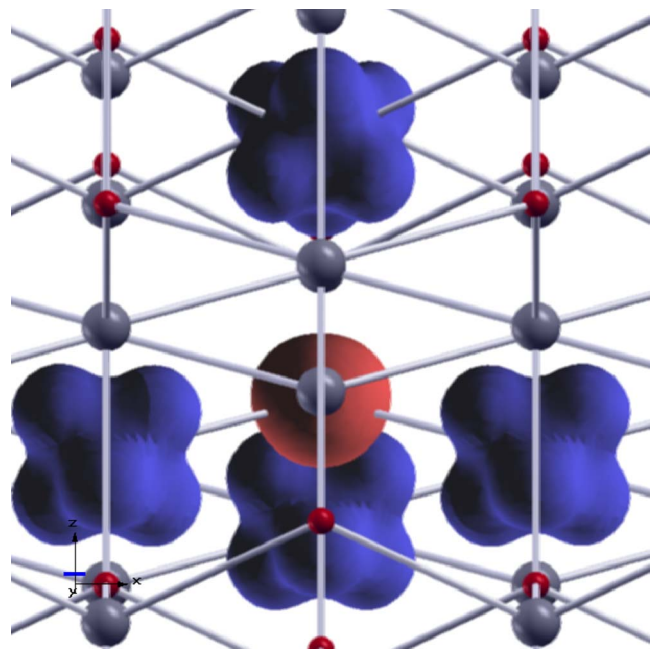


FIG. 6. (Color online) Same as in Fig. 5 but for a Co tetramer evaluated for an energy interval of 0.7 eV below the Fermi level.

#### IV. SUMMARY

In conclusion, from our *ab initio* density-functional calculations, we have obtained values of interatomic exchange interaction parameters, electronic structure, and magnetic moments, using both the LSDA and the LSDA+ $U$  methods. Our results are overall consistent with experimental observations, especially concerning the exchange interaction, where we find that the Co atoms have weak antiferromagnetic coupling inside the clusters, in particular from the LSDA+ $U$  calculations. Based on our results we argue that the LSDA+ $U$  method is more appropriate for this system than the LSDA approximation. Finally we note that the decrease in the values of the calculated formation energies as a function of cluster size indicates a strong tendency to have Co nanoclusters in the ZnO matrix.

#### ACKNOWLEDGMENTS

B.S. and O.E. are grateful to the Swedish Foundation for Strategic Research (SSF), the Swedish Research Council (VR), and the Göran Gustafsson Foundation for financial support. We also acknowledge computational support from Swedish National Infrastructure for Scientific Computing (SNIC).

\*corresponding author; biplab.sanyal@fysik.uu.se

<sup>1</sup>T. Fukushima, K. Sato, H. Katayama-Yoshida, and P. H. Dederichs, Jpn. J. Appl. Phys., Part 2 **45**, L416 (2006).

<sup>2</sup>B. Sanyal, O. Grånäs, D. M. Iuşan, O. Karis, and O. Eriksson, J.

Appl. Phys. **103**, 07D131 (2008).

<sup>3</sup>A. Barla, G. Schmerber, E. Beaupaire, A. Dinia, H. Bieber, S. Colis, F. Scheurer, J.-P. Kappler, P. Imperia, F. Nolting, F. Wilhelm, A. Rogalev, D. Müller, and J. J. Grob, Phys. Rev. B **76**,

- 125201 (2007).
- <sup>4</sup>D. Iuşan, R. Knut, B. Sanyal, O. Karis, O. Eriksson, V. A. Coleman, G. Westin, J. M. Wikberg, and P. Svedlindh, *Phys. Rev. B* **78**, 085319 (2008).
- <sup>5</sup>D. Rubi, J. Fontcuberta, A. Calleja, Ll. Aragonés, X. G. Capdevila, and M. Segarra, *Phys. Rev. B* **75**, 155322 (2007).
- <sup>6</sup>T. C. Kaspar, T. Droubay, S. M. Heald, M. H. Engelhard, P. Nachimuthu, and S. A. Chambers, *Phys. Rev. B* **77**, 201303(R) (2008).
- <sup>7</sup>S. Zhou, K. Potzger, J. von Borany, R. Grötzschel, W. Skorupa, M. Helm, and J. Fassbender, *Phys. Rev. B* **77**, 035209 (2008).
- <sup>8</sup>T. Dietl, T. Andrearczyk, A. Lipińska, M. Kiecana, M. Tay, and Y. Wu, *Phys. Rev. B* **76**, 155312 (2007).
- <sup>9</sup>O. Eriksson, D. Iuşan, R. Knut, and B. Sanyal, *J. Appl. Phys.* **101**, 09H114 (2007).
- <sup>10</sup>D. Iuşan, B. Sanyal, and O. Eriksson, *Phys. Rev. B* **74**, 235208 (2006).
- <sup>11</sup>G. Kresse and D. Joubert, *Phys. Rev. B* **59**, 1758 (1999).
- <sup>12</sup>J. P. Perdew, K. Burke, and M. Ernzerhof, *Phys. Rev. Lett.* **77**, 3865 (1996).
- <sup>13</sup>G. Kresse and J. Furthmüller, *Phys. Rev. B* **54**, 11169 (1996).
- <sup>14</sup>S. L. Dudarev, G. A. Botton, S. Y. Savrasov, C. J. Humphreys, and A. P. Sutton, *Phys. Rev. B* **57**, 1505 (1998).
- <sup>15</sup>B. Sanyal, O. Grånäs, R. Knut, V. A. Coleman, P. Thunström, D. M. Iuşan, O. Karis, O. Eriksson, and G. Westin, *J. Appl. Phys.* **103**, 07D130 (2008).
- <sup>16</sup>P. Gopal and N. A. Spaldin, *Phys. Rev. B* **74**, 094418 (2006), and references therein.
- <sup>17</sup><http://exciting.sourceforge.net>
- <sup>18</sup>I. V. Solovyev, A. I. Liechtenstein, and K. Terakura, *Phys. Rev. Lett.* **80**, 5758 (1998).
- <sup>19</sup>F. Cricchio, F. Bultmark, and L. Nordström, *Phys. Rev. B* **78**, 100404(R) (2008).
- <sup>20</sup>A. O. Shorikov, A. V. Lukoyanov, M. A. Korotin, and V. I. Anisimov, *Phys. Rev. B* **72**, 024458 (2005).
- <sup>21</sup>K. Sato, L. Bergqvist, G. Bouzerar, P. H. Dederichs, V. A. Dinh, O. Eriksson, T. Fukushima, H. Katayama-Yoshida, H. Kizaki, J. Kudrnovsky, B. Sanyal, M. Toyoda, I. Turek, and R. Zeller (unpublished).
- <sup>22</sup>A. Bergman, L. Nordström, A. B. Klautau, S. Frota-Pessoa, and O. Eriksson, *Phys. Rev. B* **73**, 174434 (2006).
- <sup>23</sup>A. Bergman, L. Nordström, A. Burlamaqui Klautau, S. Frota-Pessoa, and O. Eriksson, *Phys. Rev. B* **75**, 224425 (2007).
- <sup>24</sup>A. Walsh, J. L. F. Da Silva, and S.-H. Wei, *Phys. Rev. Lett.* **100**, 256401 (2008).
- <sup>25</sup>S. Lany, H. Raebiger, and A. Zunger, *Phys. Rev. B* **77**, 241201(R) (2008).
- <sup>26</sup>I. V. Solovyev, *J. Phys.: Condens. Matter* **20**, 293201 (2008).
- <sup>27</sup>P. Sati, C. Deparis, C. Morhain, S. Schafer, and A. Stepanov, *Phys. Rev. Lett.* **98**, 137204 (2007).
- <sup>28</sup>T. Chanier, M. Sargolzaei, I. Opahle, R. Hayn, and K. Koepf, *Phys. Rev. B* **73**, 134418 (2006).
- <sup>29</sup>M. A. White, S. T. Ochsenein, and D. R. Gamelin, *Chem. Mater.* **20**, 7107 (2008).
- <sup>30</sup>X. Y. Cui, J. E. Medvedeva, B. Delley, A. J. Freeman, N. Newman, and C. Stampfl, *Phys. Rev. Lett.* **95**, 256404 (2005).
- <sup>31</sup>V. I. Anisimov, J. Zaanen, and O. K. Andersen, *Phys. Rev. B* **44**, 943 (1991).
- <sup>32</sup>G. Ghiringhelli, L. H. Tjeng, A. Tanaka, O. Tjernberg, T. Mizokawa, J. L. de Boer, and N. B. Brookes, *Phys. Rev. B* **66**, 075101 (2002).